Cell

Tcf3 Governs Stem Cell Features and Represses Cell Fate Determination in Skin

Hoang Nguyen,[1] Michael Rendl,[1] and Elaine Fuchs[1,*]
[1] Howard Hughes Medical Institute, Department of Mammalian Cell Biology and Development, The Rockefeller University, 1230 York Avenue, Box 300, New York, NY 10021, USA
*Contact: fuchslb@rockefeller.edu
DOI 10.1016/j.cell.2006.07.036

SUMMARY

Many stem cells (SCs) respond to Wnt signaling, but whether β-catenin's DNA binding partners, the Tcfs, play a role in SCs in the absence of Wnts, is unknown. In adult skin, quiescent multipotent progenitors express Tcf3 and commit to a hair cell fate in response to Wnt signaling. We find that embryonic skin progenitors also express Tcf3. Using an inducible system in mice, we show that upon Tcf3 reactivation, committed epidermal cells induce genes associated with an undifferentiated, Wnt-inhibited state and Tcf3 promotes a transcriptional program shared by embryonic and postnatal SCs. Further, Tcf3-repressed genes include transcriptional regulators of the epidermal, sebaceous gland and hair follicle differentiation programs, and correspondingly, all three terminal differentiation pathways are suppressed when Tcf3 is induced postnatally. These data suggest that in the absence of Wnt signals, Tcf3 may function in skin SCs to maintain an undifferentiated state and, through Wnt signaling, directs these cells along the hair lineage.

INTRODUCTION

In response to Wnt signaling, β-catenin is stabilized and can associate with the Tcf/Lef1 family of DNA binding proteins to transactivate downstream target genes. Increasing evidence underscores a major role for Wnt signaling in stem cell (SC) biology (Reya and Clevers, 2005). Loss of function studies in the mouse intestine show that Tcf4 is essential for establishing epithelial crypts (Korinek et al., 1998), and gain-of-function studies suggest that Tcf4 and Wnt/β-catenin signaling act in concert to maintain the progenitor pool and inhibit differentiation (van de Wetering et al., 2002). Similarly, the Wnt/β-catenin pathway is active in the progenitor cells of the hippocampus (Lie et al., 2005). In vitro, Wnt signaling expands the pools of hematopoietic SCs (Willert et al., 2003).

While Tcfs/β-catenin signaling is important in progenitor proliferation, it is also used by SCs to specify certain lineages at the expense of others. In skin, β-catenin/Lef1 signaling promotes hair-shaft differentiation, and, at excessive levels, tumors of this cell lineage arise (Gat et al., 1998; DasGupta and Fuchs, 1999; Van Mater et al., 2003; Lo Celso et al., 2004). Analogously, elevated Wnt signaling instructs neural SCs to adopt a sensory neuronal fate (Lee et al., 2004), coaxes skeletal progenitors toward osteoblast rather than chondrocyte differentiation (Day et al., 2005), and promotes Paneth cell differentiation in the intestine (van Es et al., 2005). Whether SCs proliferate or differentiate in response to Wnt signaling is likely to depend upon factors that influence the levels and activities of Tcf/Lef1/β-catenin complexes and their associated proteins. Despite the well-established link between Wnt signaling and SC biology, however, little is known about the functional significance and the underlying mechanisms involved in this link.

Whether Lef1/Tcf proteins function in SCs in the absence of Wnt signaling is even less clear, although some evidence suggests that they can do so in other situations (Brannon et al., 1999; Cavallo et al., 1998; Roose et al., 1998; Hamada and Bienz, 2004; Shetty et al., 2005; Daniels and Weis, 2005). In *Drosophila*, for example, interaction of dTcf with the Groucho/TLE family of transcriptional repressors antagonizes Wnt/Wingless signaling (Cavallo et al., 1998). Similarly, forced Groucho/TLE expression in *Xenopus* embryos can block activation of β-catenin target genes necessary for axis formation (Roose et al., 1998). In mammalian cell lines, Lef1 has been shown to occupy a site in the *c-Myc* enhancer that is accompanied by TLE and five other chromatin repressor proteins, while stabilization of β-catenin displaces the TLE/chromatin repressor complex and recruits chromatin activators without displacing Lef1 (Sierra et al., 2006).

These findings suggest that in the absence of stabilized β-catenin, Lef1/Tcfs may be functionally important in regulating gene expression. Consistent with this notion are gene-targeting studies on Tcf3, a Lef1/Tcf family member that has been increasingly viewed as a transcriptional

repressor. In mice, *Tcf3* ablation results in gastrulation defects that resemble a Wnt gain-of-function phenotype (Merrill et al., 2004), and the headless phenotype displayed by Tcf3-deficient zebrafish is complemented by an N-terminally truncated Tcf3 lacking its β-catenin binding domain (Kim et al., 2000).

In adult skin, Tcf3 is naturally expressed in the hair-follicle bulge, which is thought to be a niche for the multipotent stem cells that are required for hair cycling and epidermal wound repair (Cotsarelis et al.,1990; Taylor et al., 2000; Oshima et al., 2001; Merrill et al., 2001). In contrast to many SC niches, the bulge maintains a sizeable pool of infrequently cycling cells, which become activated at the start of each hair growth phase. At this time, the new hair germ appears at the base of the bulge and shows Wnt reporter gene (TOPGAL) activity and nuclear β-catenin (DasGupta and Fuchs, 1999; Merrill et al., 2001). When levels of stabilized β-catenin are genetically elevated, SC activation and hair growth occur precociously (Gat et al., 1998; Van Mater et al., 2003; Lo Celso et al., 2004), and many cell proliferation-associated genes are upregulated (Lowry et al., 2005). These studies have suggested that Tcf3 might repress proliferation in the bulge and that Wnt signaling acts to stimulate SC activation.

During the growth phase of the hair cycle, Tcf3 is expressed not only in the quiescent bulge SCs but also in the outer basal layer of the newly formed outer root sheath (ORS) (DasGupta and Fuchs, 1999). These cells are thought to represent mobilized SCs on route to the base of the hair follicle (Oshima et al., 2001; Vidal et al., 2005). An ORS/bulge morphology can be achieved by expressing Tcf3 in the epidermis of transgenic mice, suggesting that Tcf3 may specify some of these characteristics (Merrill et al., 2001). Interestingly, the same phenotype can be obtained by expressing ΔNTcf3 lacking the β-catenin interacting domain, suggesting that Tcf3 might function independently of Wnt signaling in determining these features (Merrill et al., 2001).

The questions of whether and how Tcf3 functions to regulate gene expression in follicle SCs reside at the nexus of defining the physiological importance of Tcfs and Wnt signaling in SC and cell lineage determination. To resolve this issue, we first showed that Tcf3 is expressed in early embryonic skin, which is composed of multipotent progenitors, and that it is downregulated concomitant with fate specification. We then engineered mice that enable us to control the expression of Tcf3 and either sustain it embryonically or switch it back on postnatally. We then conducted microarray profilings and molecular analyses, which reveal Tcf3 as a key transcriptional regulator of both embryonic and adult skin progenitors. We show that, surprisingly, Tcf3 temporally represses transcriptional regulators of epidermal and sebaceous gland differentiation, two lineages not known to be regulated by Wnt signaling. Finally, we demonstrate that when the Tcf3 signature is applied to postnatal epidermis in vivo, all three programs of terminal differentiation are repressed and the epithelium transforms into a relatively undifferentiated state that resembles that of stem cells.

RESULTS

Tcf3 Is Expressed in Proliferating, Unspecified Embryonic Epidermal Progenitors

If Tcf3 is truly an indicator of progenitor status in the skin, it should be expressed not only in adult bulge SCs but also in unspecified embryonic epidermis. To test this possibility, we used a monospecific Tcf3 antibody (Merrill et al., 2001) and examined E13.5 epidermis, which exists as a single layer of multipotent progenitor cells that express the keratinocyte-specific marker keratin 5 (K5). Anti-Tcf3 localized to the nuclei of these progenitors, which colabeled with antibodies against proliferating nuclear antigen, Ki67 (Figures 1A and 1B). This contrasted with the inverse relation observed between Tcf3 and Ki67 in the bulge (DasGupta and Fuchs, 1999; Blanpain et al., 2004).

As development proceeded, Tcf3 progressively waned, and by P1, it was no longer detected in the epidermal basal layer. In developing hair follicles, Tcf3 was first detected in a small cluster of cells located in the ORS (Figure 1A, brackets). This site coincided with the base of strong anti-β4 integrin staining, i.e., below the site at which the sebaceous gland will bud, at or shortly after birth. Notably, this position also corresponded to the future site of the follicle bulge, a multipotent SC reservoir in postnatal skin (Blanpain et al., 2004). This intriguing finding suggested that the adult SC compartment is established early, at a time when the progenitor cells in the basal layer of the epidermis become more restricted and cease de novo hair follicle morphogenesis.

Postnatally, the zone of Tcf3(+) cells in anagen-phase follicles expanded downward along the ORS (Figure 1C, P1–P5). Many but not all of these Tcf3(+) cells were Ki67(−). Conversely, most Ki67(+) cells in the follicle were Tcf3(−). This was especially true for the Mx cells at the base of the follicle. Figure 1D summarizes the expression data. When taken together with our prior studies in postnatal skin (DasGupta and Fuchs, 1999; Merrill et al., 2001), these findings support the view that Tcf3 is expressed in skin progenitor cells, whether they are embryonic and proliferative or postnatal and quiescent.

Identifying the Genes whose Expression Is Affected following Tcf3 Induction

To understand Tcf3's role in epidermal progenitor cells, we first needed to identify the genes that are affected by its expression. To this end, we devised a strategy to control Tcf3 levels in postnatal basal epidermal cells that are committed and have turned off endogenous Tcf3 expression. We began by engineering ten founder mice to express the tetracycline-sensitive transactivator, rtTA2S-M2-VP16 (rtTA), under the control of the *keratin 14* (*K14*) promoter active in embryonic and postnatal basal cells (Vasioukhin et al., 1999; Knott et al., 2002) (Figure 2A). The most tightly regulated transactivator mouse was

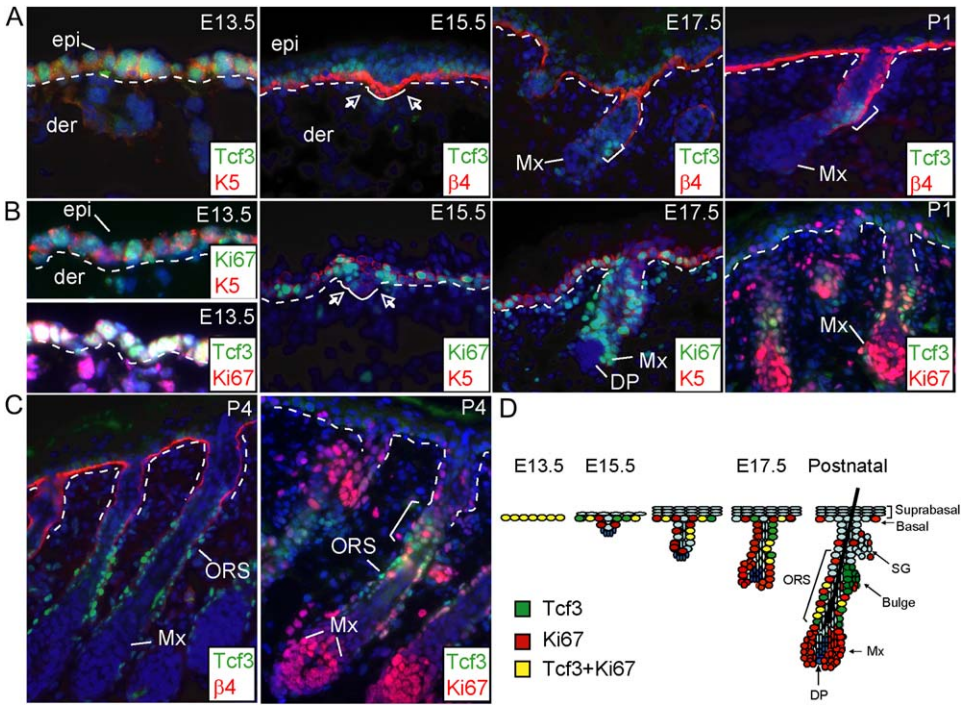

Figure 1. Expression of Tcf3 during Embryonic Epidermal Development

(A)–(C) Immunofluorescence microscopy of frozen skin sections (10 μm) from mice at ages indicated in upper right. Abs are color coded according to secondary Abs noted in lower right. Dapi (blue) was used to counterstain nuclei. K5 is a pan marker of keratinocytes, β4 integrin is a component of hemidesmosomes, and Ki67 is a proliferative nuclear antigen. Epi abbreviates epidermis, der stands for dermis, white dotted lines denote dermo-epidermal border, ORS stands for outer root sheath, Mx abbreviates matrix, DP denotes dermal papilla, and SG stands for the sebaceous gland. Arrows denote hair placodes; brackets denote Tcf3-positive nuclei at site of the future bulge.

(D) Schematic summarizing embryonic skin development and Ki67 and Tcf3 expression patterns (yellow denotes coexpression).

then mated to a second line engineered to express *Tcf3* under the control of a tetracycline regulatory element (*TRE*). To distinguish transgenic from endogenous Tcf3, we used an amino terminal C-myc epitope tag, previously shown not to interfere with Tcf3 function in vivo (Merrill et al., 2001).

Mice doubly transgenic for *K14-rtTA* and *TRE-mycTcf3* exhibited strict tetracycline (doxycycline, Dox)-mediated regulation of mycTcf3 (Figure 2B). Within 3 hr after Dox injection, mice expressed Tcf3 throughout the epidermis, follicle ORS, and sebaceous glands, and by 24 hr, expression was maximal. Soon after (~48 hr), phenotypic changes began to appear, which are addressed below. By immunofluorescence, induced Tcf3 levels in the basal layer appeared to reach a maximum by ~10–12 hr following Dox administration. To quantify the induction levels, we FACS-purified basal cells from embryonic, Tcf3-uninduced, and Tcf3-induced (10 hr) neonatal epidermis and performed immunoblot analyses on equal numbers of basal cells. As shown in Figure 2C, the overall levels of induced Tcf3 rose to three to four times the endogenous levels found in embryonic epidermis. Moreover, the Tcf3 protein generated by transgene expression was of the expected size.

Primary epidermal keratinocytes (MK) cultured from these mice showed similar kinetics of induction, following addition of Dox to the medium (Figure 2D). By immunoblot analyses, Tcf3 was not detected in uninduced MK, but within 3 hr after induction, the protein was readily detected (Figure 2E).

To identify the genes affected by Tcf3, we performed microarray analyses on isolated epidermal mRNAs purified from mice that were injected with Dox for 6, 12, and 24 hr. One hundred and fifty genes scored as ≥2× up- or downregulated within 6 hr after Dox induction of Tcf3 expression, and by 12–24 hr, this number rose to ~300 genes (Figure 2F). Table S1 provides comprehensive lists of the ≥2× up- and downregulated probesets. Table 1 lists Tcf3-affected genes which were analyzed further. Since gene repression must overcome endogenous levels of mRNAs which vary in stabilities, we also included a few genes known to be relevant to skin epithelial lineages but whose probesets scored as only 1.9× downregulated.

To further verify these Tcf3-induced changes and further explore their kinetics, we performed real-time PCR analyses on independent mRNA populations from the epidermises of transgenic mice treated with Dox for 0, 6, 12, 24, and 50 hr (Figure S1). Overall, expression patterns were similar to the results obtained by microarray analyses. Changes in expression of many of these genes were rapid, initiating within 6 hr of Dox administration. Notably,

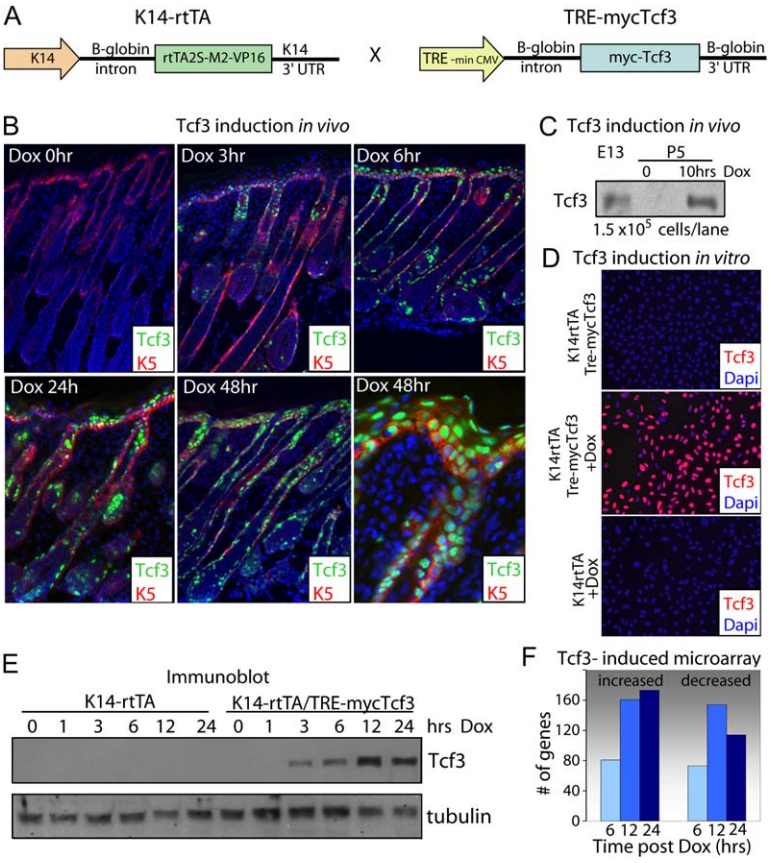

Figure 2. Generation of Transgenic Mice Able to Induce Tcf3 in Skin Epithelium in Response to Doxycycline

(A) Constructs used to generate transgenic mice expressing skin epithelial-specific Tcf3 under the control of doxycycline (Dox).

(B) Tcf3 induction in vivo. *K14rtTA/TRE-mycTcf3* mice were injected intraperitoneally with Dox for the times indicated prior to reaching 4 days of age. At P4, backskins were frozen, sectioned, and subjected to immunofluorescence microscopy using the Abs indicated (color coding according to secondary Abs). Second 48 hr Dox frame is at higher magnification.

(C) Anti-Tcf3 immunoblot of protein extracts isolated from equal numbers of FACS-purified basal cells from backskins of E13.5 embryos and P5 transgenic mice either uninduced (0 hr) or induced for 10 hr with Dox.

(D) Tcf3 induction in vitro. Primary mouse keratinocytes (MK) isolated from double or single transgenic mice were cultured ±100 ng/ml Dox for 24 hr, followed by immunostaining for Tcf3 (red) and Dapi (blue).

(E) Immunoblot analyses of Tcf3 induction in vitro. Total protein lysates were prepared from MK exposed to Dox as indicated. Immunoblots were probed with Abs against Tcf3 (test) and tubulin (control for loadings).

(F) Numbers of genes up- and downregulated following Tcf3 induction in vivo. mRNAs were isolated from Tcf3-induced skins from (B) and subjected to microarray analyses. Shown are the overall numbers of genes whose expression changed by $\geq 2\times$.

genes involved in lipid metabolism and electron transport were preferentially suppressed by Tcf3, while genes involved in carbohydrate metabolism, energy pathways, and cell motility were preferentially induced (Figure S1, graph C). Marked changes, both up- and downregulated, were also observed in genes involved in signal transduction, cell growth, and maintenance.

The Tcf3-Signature Is Similar to the Bulge/ORS Signature but Divergent from Signatures of Transit-Amplifying Basal Epidermal and Matrix Cells

Since Tcf3 correlated with epidermal progenitor status, we first compared our Tcf3 signature with previously published bulge signature genes (Legg et al., 2003; Tumbar et al., 2004; Blanpain et al., 2004; Morris et al., 2004). As Tcf3 levels increased, similarities between Tcf3 and bulge signatures also rose (Figure 3A). This was true for both Tcf3-induced and Tcf3-repressed signature genes. The similarities between bulge and Tcf3-induced signatures were documented by comparing the expression levels of these genes in purified populations of Tcf3(+) bulge SCs (α6highCD34+K14+) relative to Tcf3(−) basal epidermal cells (α6lowCD34−K14+). Figure S2 provides representative examples delineating these marked similarities.

To more fully ascertain the potential significance of the overlap between Tcf3 and bulge signatures, we devised strategies to isolate, purify, and transcriptionally profile the proliferative cells of P5 epidermis, follicle matrix, and ORS. When cross-compared, a molecular signature was obtained identifying the distinguishing features for each population. We then determined the degree to which Tcf3-induced and -repressed genes overlapped with these three new signatures. The results show clearly that as Tcf3 levels rose, the induced gene pattern became increasingly similar to the ORS signature, while genes repressed by Tcf3 were typically features of the epidermal signature (Figure 3B). Neither Tcf3 signature showed similarity to the matrix gene expression pattern (Figure 3B). These data document the specificity of the signature that was generated by Tcf3 induction in the skin. Moreover, the data reveal that the Tcf3 signature faithfully parallels the molecular distinctions that naturally occur between Tcf3(+) follicle ORS/bulge and the so-called transit amplifying cells of the epidermis and hair follicle. A full list of all Tcf3-induced and -repressed genes sharing similarities with the bulge, ORS, and epidermis is provided in Table S2.

Identifying Genes Associated with Progenitor Status Irrespective of Proliferative State

Despite interesting parallels, certain facets of the bulge signature were distinct from the Tcf3-induced epidermal

Table 1. Genes Induced or Suppressed following Tcf3 Induction

mRNAs Induced by Tcf3	
Acy3(7.5), **Air**(2.1), **Ak1**(2.5), Angptl4(7.5)*, **Apeg1**(2.8), **Bcl2l11**(2.1), Bcor(2.3), **Bmp6**(3)*, Bmf(2.1)*, **Cdkn1c-p57**(3.7), Cldn7(8), Cldn3(2), **Cspg4**(2), **Ctsz**(2.5), Edn2(4)#, **Fgf11**(2.8), Hic2(3), **Igfbp6**(2), Insl6(2.5), Klf9(2) #, **Krt2-8**(11.3), Krt1-16 (7), Krt1-18 (4.6), Krt2-7(3.2), Krt2-17(26), Lcn2(8.6), **Ndrg1**(2.1), **Npdc1**(2.6), P2rx4(2.1), **Pcbp4**(2.1), Ptger1(6.5), Ptprs(2), **Rhoc**(3.2), Slc2a6(13), Smarcd3 (2.3), Snai3(2.3), **Sncg**(2), **Tbx1**(2.1)*, Tcfcp2l1(2.3), Tle6(2.3)#, **Zdhhc2**(7)	
mRNAs Repressed by Tcf3	
Lipid Metabolism/Epidermal Barrier Formation	**Acsl1**(2.1), **Acsl4**(2.1), Adh7(2.1), Akr1d1(4), Alox12(2.3), **Alox12e**(2.5), Edg8(2.3), Elov5(1.9), **Elovl6**(2.5)*, Faah(1.9)#, Fa2h(5.7)#, Galnt7(2.5), Gal3st1(2), Ipmk(2), **Itpr2**(2.1), **Lpl**(2.1)#, **Lrp4**(2.5), **Mgll**(2.1)#, Mlstd1(4.6), Mrc2(5.7), Palmd(2.3), **Pank1**(2.3), Panx3 (5.3), Pctp(3), Pld1(2), Pla2g4a(2.1)#, Pnpla5(2.1), **Ptgs1**(3)#, **Satb1**(2)&, **Soat1**(2.6)#, **Ugt1a2**(2.1)
Transcription/Nuclear Factors	**Klf5**(1.9)*, **Mlze**(3.5)*, Peli1(2.5), PPARγ(4)*, **Pou3f1**(2), **Satb1**(2)&, Trp63(2.8)
Wnt Signaling/Targets	**Axin2**(2.1)*, **Ccnd2**(1.9)*, Dkkl1(2.5), Scube2(2.6), Sostdc1(5.3)*, **Tnfrsf19**(1.9)
Adhesion/Migration	Col8a1(2.1), **Daf1**(2.3), Leprel1(2.5), Mmp2(2.1)* Nck1(2.1), Npnt(2), Pcdh20(2), Rgmb(2.3)*, Sema3c(2.3), Serpinb12(3.7), Slitrk6(3), **Tmprss4**(2), Tnc(1.9)
Growth Signaling/Cytokines	Adora2b(2.6), Ccl27(3.2), **Ccrl1**(5.3)*, Cd36(2.6), **Fgfbp1**(1.9), **Fgf13**(1.9), Igfbp2(2)*, Il1f5(2), **Il1r2**(2.1), Irs1(2)&, Lmyc1(3.5)*, Nedd9(2)*, **Pdgfc**(2.6)*, Popdc3(2.6), Ppp1r14c(2.6), **Ptgs1**(3)#, Rab27a(2.3), Rgs12(2.1), **Rgs18**(1.9), **Satb1**(2), **Sdpr**(2)
Hormone Signaling/Biosynthesis	**Dio2**(2.5), Hsd3b6(4), Pxmp4(2.1), Rbp2(2.1), Rdh1(2.3), **Rdh9**(2.1), **Rdh11**(2.5)

K14rtTA (control) and *K14rtTA/TRE-mycTcf3* mice were injected intraperitoneally with 100 μg Dox for 6, 12, and 24 hr prior to harvesting at P5. Backskin epidermises were then removed enzymatically by dispase, RNAs were isolated, and microarray analyses were performed. *K14rtTA/TRE-mycTcf3* and *K14rtTA* arrays were compared as described in the Supplemental Experimental Procedures. Data from the relevant gene categories are shown, with fold up- or downregulated given in parentheses. Numbers in parentheses indicate maximal fold increase or decrease within 24 hr after Dox. Genes in bold font show similar patterns of expression with known bulge signatures.

* Denotes genes with conserved TCF and PPAR binding sites within 10 kb of the transcription initiation site.

# Denotes genes with conserved PPAR binding sites within 10 kb of the transcription initiation site.

& Denotes genes with conserved TCF binding motifs within 10 kb of the transcription initiation site.

signature. Most notably, of the myriad of cell-cycle regulatory genes that were differentially expressed in quiescent versus activated bulge cells (Tumbar et al., 2004; Lowry et al., 2005), only *Cdkn1c (p57)* and *Ccnd2 (cyclin D2)* were similarly affected in Tcf3-induced epidermis. Thus, the majority of the transcriptional differences in cell-cycle regulated genes within the bulge appeared to mirror their slow-cycling nature rather than Tcf3-expression status.

To identify which of the Tcf3-signature genes correlate with progenitor rather than proliferative status, we examined the developmental expression patterns of a group of Tcf3-sensitive genes that were also represented in the bulge signature. Notably, the ones upregulated in both Tcf3-induced and bulge signatures were also highly expressed in E13.5 skin, and they were more poorly represented at later embryonic stages (Figure 4A). This correlation held when mRNAs were examined from FACS-purified E13.5 and P5 basal cells (Figure 4B). Conversely, those genes downregulated by Tcf3 tended to be weakly expressed at E13.5 and upregulated during development (Figures 4C and 4D).

Tcf3 Induction Leads to PPAR Repression

Among the most strongly repressed genes in the Tcf3 array encoded peroxisome proliferator-activated receptors (PPARs). Real-time PCR further established that both *PPARγ* and *PPARα* were repressed following Tcf3 induction, and their expression was also reduced in the bulge (Figures S1 and S2). This finding was particularly interesting given that the PPAR transcription factors are involved in epidermal and sebaceous gland differentiation, respectively (Di-Poi et al., 2004). Moreover, in adipocytes, PPARγ regulates a number of genes involved in the synthesis and production of lipids, many of which were also repressed in our Tcf3-induced array (Tables 1, S1 and S2; Figure S1C). Accounting for >10% of the Tcf3-repressed signature, these lipid-related genes were also expressed at considerably higher levels in Tcf3(−) P5 basal cells than in Tcf3(+) E13.5 basal cells, underscoring their importance in epidermal differentiation and barrier function acquisition (Figure 4D).

The inverse correlation between *Tcf3* and *PPAR* gene expression was also reflected at the level of immunofluorescence microscopy (Figure 5A). Nuclear PPARα was detected in differentiating cells of the epidermis, while PPARγ was found in differentiating sebocytes. Upon Tcf3 induction, expression of both PPARα and PPARγ waned. In addition, neither PPARs were detected in E13.5 epidermis (Figure 5B). PPARγ expression occurred later, concomitant with sebaceous gland differentiation, as marked by Oil-red O staining. At P1, the initial zones of PPARγ and Tcf3 expression were adjacent but mutually exclusive

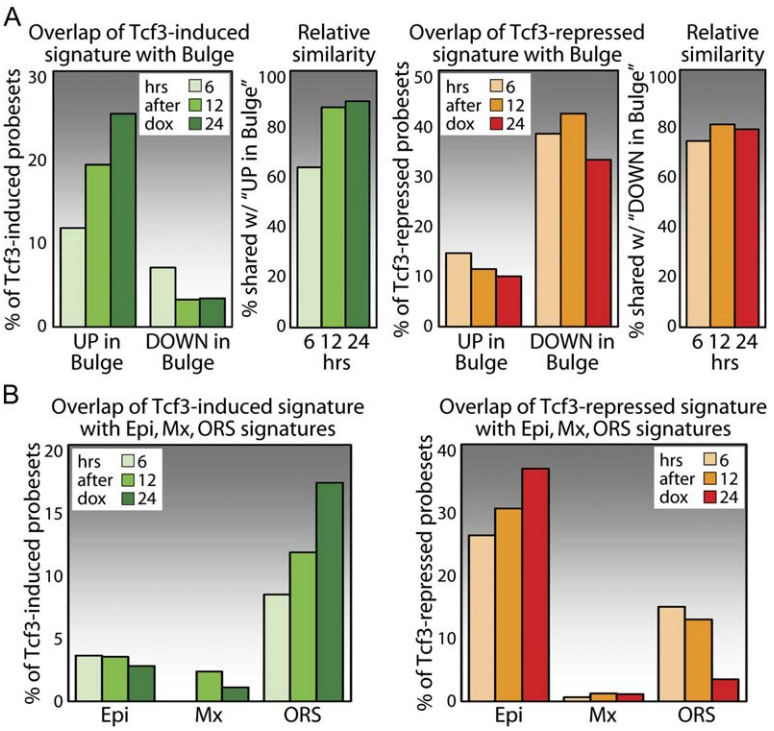

Figure 3. With Times after Tcf3 Induction, the Tcf3 Signature Increasingly Resembles the Bulge and ORS Signatures

(A) The Tcf3-induced (green tones) and Tcf3-repressed (red tones) signatures are compared with genes that are either up- or downregulated in the bulge relative to basal skin epithelial cells. Note that with times after Tcf3 induction, the overlap between these signatures increases. The relative similarities between the Tcf3-induced and the "UP in bulge" signature (green) and between the Tcf3-repressed and the "DOWN in Bulge" signature (red) are shown at right as percentage of all similarities.

(B) The Tcf3-induced and -repressed signatures were compared to the signature genes that distinguish P5 epidermal (Epi), hair follicle matrix (Mx), and outer root sheath (ORS) cells. Note that the similarities are greatest between Tcf3-induced genes and the ORS signature, and also between Tcf3-repressed genes and the Epi signature.

(bracket), consistent with Tcf3 as a marker of the presumptive site of the bulge (see Figure 1).

The promoters for *PPAR* genes have Tcf3/Lef1 sites (Table 1), and several recent studies posit that Wnt and PPAR signaling pathways may be intertwined (Saez et al., 2004; Liu and Farmer, 2004; Jansson et al., 2005; Kang et al., 2005). A survey of the Tcf3-suppressed lipid genes in our array revealed putative PPAR-RXRα binding motifs in many of their promoters (denoted by the pound sign [#] in Table 1). Based upon these analyses, the Tcf3 signature could be viewed as an assembly of genes, some of which possess putative Tcf3/Lef1 binding sites, while others feature PPAR/RXRα binding motifs. A few genes contained putative binding sites for both Tcfs and PPARs (see Table 1).

It was notable that like *PPAR*γ and *PPAR*α, many established Wnt target genes, e.g., *Axin2*, *Dkkl1*, and *Ccnd2* (*Cyclin D2*), exhibited rapid repression within 6 hr of Tcf3 treatment, while some bona fide PPAR target genes such as *Lpl, Pla2g4a, Ptgs1* and *Faah* displayed delayed kinetics of repression (see Figure S1B, Table S1). To address whether *PPAR* genes might be direct targets for Tcf3-mediated repression, we cultured transgenic MK. In the absence of Dox, these cells did not express appreciable Tcf3 but did express *PPAR*γ, *PPAR*α, and *PPAR*δ mRNAs. *PPAR*γ displayed the greatest sensitivity to Tcf3 induction (Figure 5C).

A conserved Lef1/Tcf consensus binding motif resides within 6 kb of the transcription initiation sites for each of the *PPAR* genes. These sites appeared to bind Tcf3 directly, as judged by chromatin immunoprecipitation (ChIP) assays performed on MK treated with Dox for 3 hr. Only after Tcf3 induction were ChIP complexes detected that contained (1) Tcf3 and (2) the sequences that encompassed the most highly conserved putative Lef1/Tcf binding sites in the *PPAR* promoters (Figure 5D). These complexes were obtained with antibodies against either Tcf3 or the C-myc epitope tag (shown). By contrast, these antibodies did not immunoprecipitate DNA from promoter regions that lacked putative Tcf/Lef motifs (con). Similar results were obtained with *Klf5* and *Bmp6* genes, suggesting that Tcf3 could bind to promoters of induced as well as repressed genes (Figure 5D).

To verify that endogenous Tcf3 binds to these genes, we repeated the ChIP assays with chromatin isolated from P5 hair follicles, which express Tcf3 in the ORS cells and uninduced P5 epidermis, where Tcf3 was not detected. Endogenous Tcf3 ChIP complexes were detected in the hair fraction for the *PPAR*γ, *PPAR*α, *KLF5*, and *Bmp6* genes (Figure 5E). As judged by the lack of complexes in the control promoter fragments, these complexes appeared to be specific for the promoter fragments harboring the putative Tcf3 binding sites. Tcf3 ChIP complexes were not detected in the epidermal fraction for either control or test fragments (shown).

Although the *PPAR* promoters are complex, the Tcf3 sites also appeared to be functionally important, as judged by *PPAR*γ*-luciferase* assays. As noted previously (Merrill et al., 2001), some species-specific variations in Tcf/βcatenin activity assays were seen, which is not surprising given the number of chromatin-associated proteins involved in activation and repression (Sierra et al., 2006).

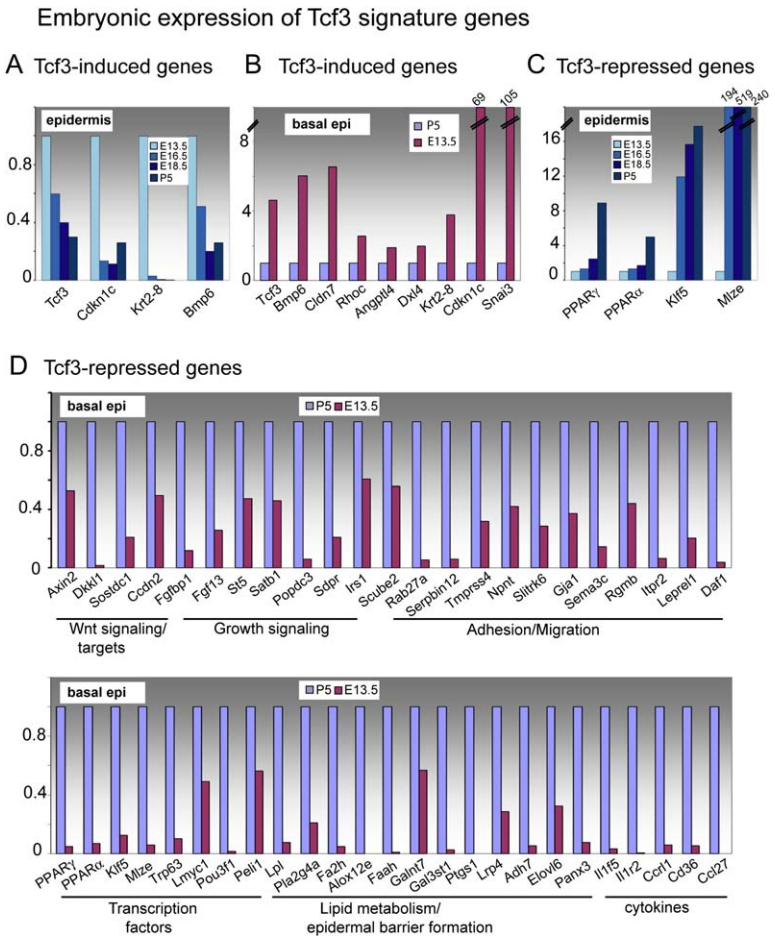

Figure 4. The Tcf3 Signature Is Shared by Early Tcf3(+) Embryonic Skin Progenitors but Is Lost during Development and Cell Fate Specification

Real-time PCR reveals a marked inverse correlation in expression of Tcf3-signature genes during embryonic skin development. mRNAs are from (A and C) total skin (E13.5) and dispase-isolated epidermis (E16.5, E18.5, P5); and (B and D) FACS-purified integrinα6(+)(K14-GFP+) basal cells from dispase-treated E13.5 and P5 skin. Genes assayed by real-time PCR are those strongly up- or downregulated upon Dox induction of Tcf3.

PPARγ-promoter activity was sensitive to Tcf3/β-catenin, and mutation of the canonical Tcf3 binding site diminished the response (Figure 5F). Conversely, β-catenin with dNTcf3 could not activate *PPAR*γ-promoter activity in mouse keratinocytes, and in human keratinocytes, Tcf3 alone repressed *PPAR*γ-promoter activity (Figure 5F).

Our results suggested that Tcf3 might be at the apex of a cascade that leads to *PPAR* suppression and subsequently the repression of epidermal and sebaceous gland differentiation pathways. To explore this notion further, we examined the effects of Tcf3 and PPARs on Tcf3-responsive genes *PPAR*γ, *PPAR*α, and *L-myc* and on the established PPARγ target gene, *lipid phospholipase* (*Lpl*) (Kim and Spiegelman, 1996; Schoonjans et al., 1996; Tachibana et al., 2005) (Figure 5G). To sustain high levels of PPARs in the presence of Tcf3, we infected Tcf3-inducible MK with retroviral vectors expressing either PPARγ (MSCV) or PPARα (pBabe). To activate PPARγ, we used the PPARγ agonist ciglitazone (Cig), which is known to stimulate expression of barrier-specific components in the epidermis as well as the sebaceous gland (Man et al., 2006). PPARα but not a mutant PPARα showed activity in MK in the absence of exogenously added ligand.

Induced Tcf3 levels were not affected by retroviral expression of PPARs or by treatment with ligand, and the levels of retrovirally expressed PPARs were sufficiently high to overcome the Tcf3-mediated suppression of their endogenous counterparts (Figure 5G). Endogenous transactivation of *Lpl* was enhanced by nearly 60× in retroviral PPARγ-expressing cells treated with ciglitazone and by ~6× with retroviral PPARα. Most importantly, by elevating the levels of active PPARs, we were able to override most of the repressive effects exerted by Tcf3 on *Lpl* expression. Based upon these findings, the ability of Tcf3 to repress *Lpl* expression appeared to be partially if not fully due to the ability of Tcf3 to repress endogenous *PPAR* expression. In contrast, *L-myc* expression was not altered appreciably by PPARs, but it was strongly repressed by Tcf3. Overall, these studies support the existence of a cascade of events linking Tcf3 to repression of a number of early differentiation-specific transcription factors including PPARs.

Repression of All Three Skin Differentiation Pathways upon Tcf3 Induction

The epidermal morphology obtained earlier with *K14-Tcf3* and with *K14-ΔNTcf3* (Merrill et al., 2001) was recapitulated upon Dox administration, but the effects were even more striking than previously realized. Epidermal differentiation was severely diminished both morphologically

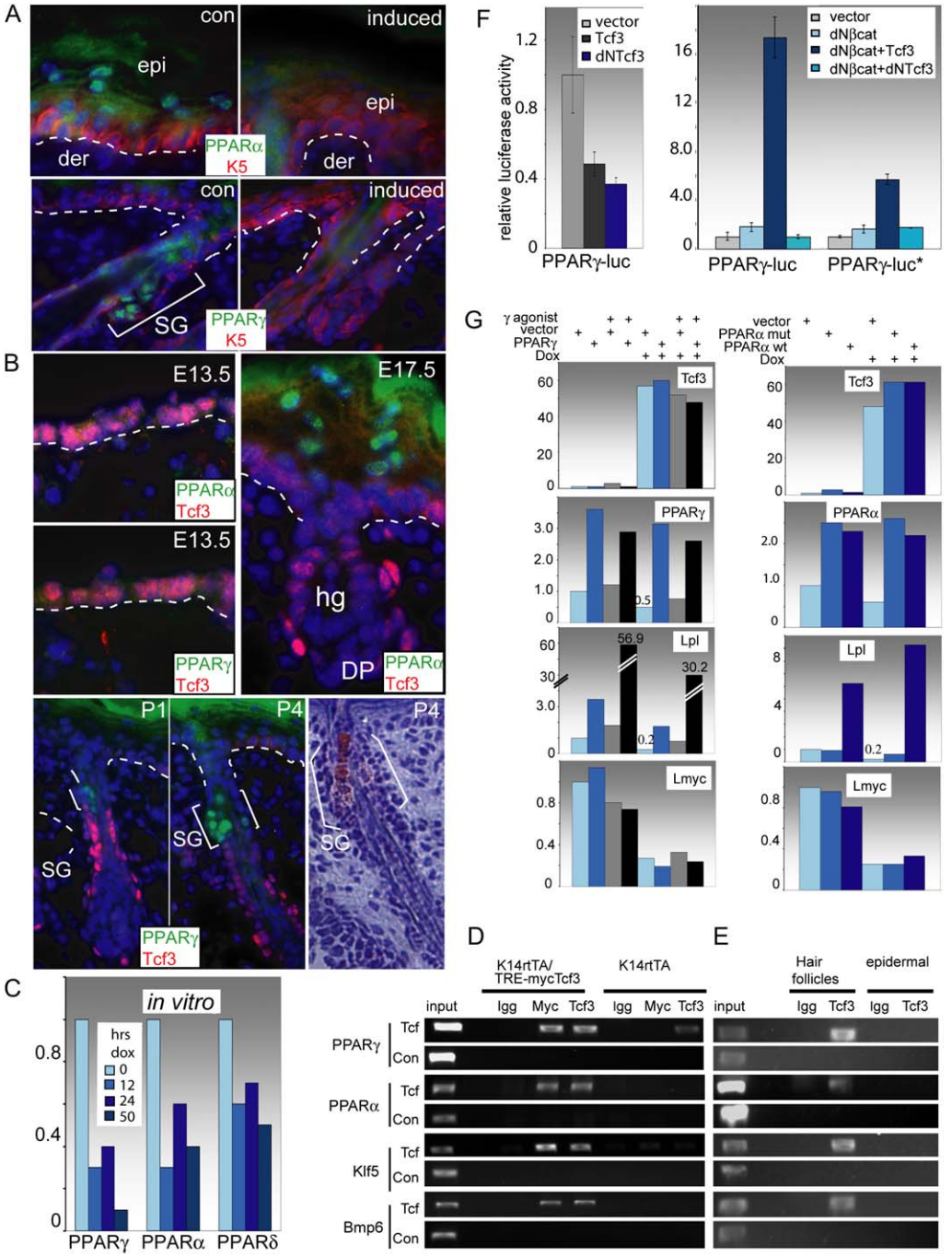

Figure 5. Tcf3-Mediated Repression of Genes Encoding PPARs, which in turn Govern Genes Involved in Lipid Synthesis/ Metabolism

(A) Tcf3 represses PPARα and PPARγ expression in skin. *K14rtTA* (control) and *K14rtTA/TRE-mycTcf3* (induced) mice were treated with Dox beginning at P1 and then processed for immunofluorescence microscopy at P5 using Abs against PPARα, PPARγ, and K5. SG denotes sebaceous gland (brackets), hf stands for hair follicle; epi stands for epidermis, and der denotes dermis. White dotted line demarcates dermo-epidermal border.

(B) Expression of PPARα and PPARγ during normal skin development. Hg, hair germ; DP, dermal papilla.

(C) Tcf3 represses PPARs *in vitro*. Real time PCR of *K14rtTA/TRE-mycTcf3* keratinocytes (MK) treated with Dox to induce Tcf3 for times indicated. *PPAR* mRNAs tested were previously reported to be expressed in vitro.

(D) In vitro ChIP. Chromatin immunoprecipitations (ChIPs) were performed on MK before and after 3 hr treatment w/Dox to induce Tcf3. Igg, control, myc-epitope and Tcf3 Abs were used for ChIP. Primer sets encompassed either the putative Tcf/Lef binding site (Tcf) or an upstream sequence lacking a consensus Tcf site (con) in each test gene. Note direct binding of Tcf3 and myc-epitope Abs only to fragments harboring Tcf3 consensus sites. Note Dox-induced Tcf3 specifity for the ChIP, consistent with the lack of appreciable Tcf3 in MK.

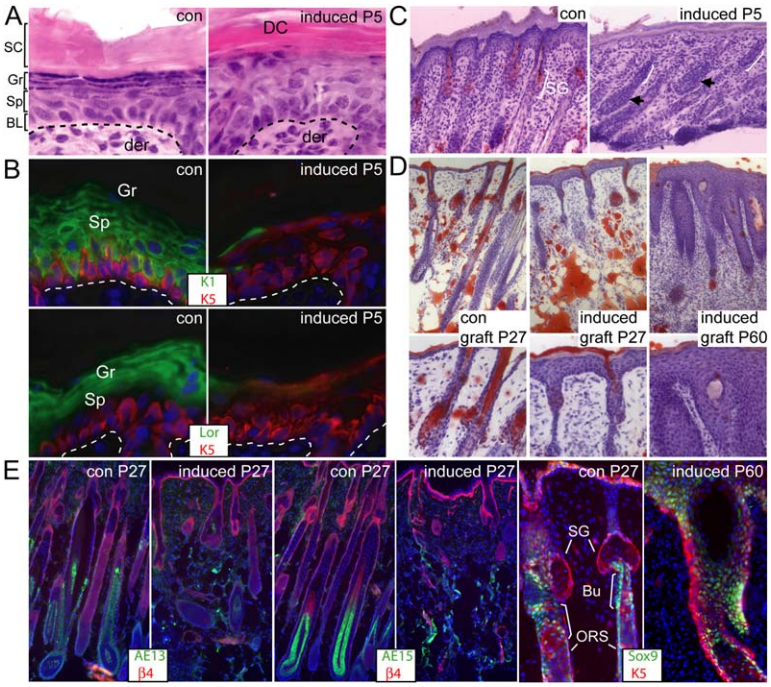

Figure 6. Tcf3 Induction Inhibits All Three lineages of Skin Development

(A and B) Repression of epidermal differentiation. P1 *K14-rtTA* (control) or *K14-rtTA/Tre-mycTcf3* (induced) mice were injected with Dox for 4 days, and tissues were either fixed, embedded, and sectioned for H&E or frozen and sectioned for immunofluorescence microscopy with the Abs indicated (color coding according to secondary Abs). Dapi (blue) was used to counterstain nuclei. The following abbreviations were used: BL, basal layer; Sp, spinous layer; Gr, granular layer; SC, stratum corneum. Note: More detailed analyses indicate that epidermal differentiation is quantitatively repressed; the squame-like structures at the surface of Tcf3-induced skin are dead cells (DC) (Figures S3 and S4).

(C) Repression of sebaceous gland development. Oil red O marks the sebaceous glands, missing in Tcf3 skin. Impairment was also observed after 2 days Dox (not shown). Note stunted downgrowth of hair follicles in induced skin (arrows).

(D) Repression of hair follicle development. Skins from *K14-rtTA* and *K14-rtTA/Tre-mycTcf3* newborn mice were grafted onto *Nude* mice, and Tcf3 was induced by Dox for the times indicated. Oil red O revealed subcutaneous fat (K14-promoter negative) but an absence of Tcf3-induced lipid-rich sebocytes (K14-promoter positive). Note that follicles, which are established embryonically (i.e., prior to Tcf3 induction), do not reinitiate the hair cycle as control follicles do but retain residual invagination. By 60 days, masses of relatively undifferentiated cells are seen, dispersed with DC pockets.

(E) Immunofluorescence reveals a block in IRS and hair-shaft differentiation but an expansion of cells positive for Sox9, a functionally important SC marker expressed in the bulge and ORS (Vidal et al., 2005).

and biochemically within 4 days after Dox (Figures 6A, 6B, S3, and S4). Ultrastructurally, the thick bundles characteristic of spinous layer K1/K10 filaments were barely detectable, and this was accompanied by a marked reduction in anti-K1/K10 immunofluorescence. Keratohyalin granules, loricrin and involucrin were also dramatically reduced. Flattened squames were present at the skin surface, giving a pretense of a stratum corneum (Figure 6A). Ultrastructurally, however, these cell remnants appeared to be dead keratinocytes rather than the end products of terminal differentiation, as they lacked the diagnostic organized lipid bilayers of stratum corneum (Figure S4). Based upon these analyses, we ruled out the possibility that Tcf3 might merely delay epidermal development.

By inducing Tcf3 postnatally, we discovered that unexpectedly, Tcf3 also dramatically impaired the other two differentiation programs in skin. The end stage of sebaceous gland differentiation can be detected by oil red O staining, which labels lipid rich sebocytes (Figure 6C, control). Within 48 hr after inducing Tcf3, however, oil red O staining was reduced, and by 4 days, it was absent. The impairment of sebaceous gland development coincided with the rapid disappearance of PPARγ detected earlier.

Specification of hair follicles occurs by birth, but their maturation is not complete until P9. As shown in Figure S3C, follicle downgrowth appeared to arrest following induction of Tcf3. To circumvent the secondary weight-loss effects that arise from Tcf3 deficiency in oral epithelia (Figure S6), we grafted P1 skins. By d27, control (con) follicles that were formed during embryogenesis had undergone degeneration and reentered the growth phase (Figure 6D, left panels). The specified follicles present at

(E) In vivo ChIP. ChIP was as in (D), except on lysates from epidermis (Tcf3-negative) and hair follicles (Tcf3-positive outer root sheath).

(F) *PPARγ* luciferase reporter assays. Luciferase reporter constructs were engineered to contain a 6 kb fragment of the mouse PPARγ promoter ± a mutation in the consensus Tcf3 binding site. Mouse Keratinocytes (MK) or Human Keratinocytes (HK) were transfected with vectors expressing Tcf3, β-catenin or ΔNTcf3 (lacking the β-catenin interacting site). Note repression of the *PPARγ* promoter by Tcf3 and the Tcf3-dependent activation of the *PPARγ* promoter by β-catenin. As reported (Merrill et al., 2001), Tcf3-dependent repression is best visualized in HK, presumably because of differences in associated chromatin-repressor proteins (Sierra et al., 2006).

(G) Direct versus indirect action of Tcf3. *K14rtTA/TRE-mycTcf3* MK were treated with the PPARγ agonist ciglitazone or Dox (Tcf3-induction) as indicated, and either infected with retroviruses expressing PPARγ, PPARα (test), mutant PPARα or empty vector (control). Real time PCR reveals dependency of *Lpl* but not *L-myc* on the status of PPARs. Note ability of retrovirally expressed PPARs to overcome Tcf3 repressive effects on endogenous *PPAR* gene expression. The error bar was calculated as the SEM.

the time of Tcf3 induction had also undergone degeneration, but in the presence of Tcf3, these follicles failed to reenter the hair cycle (Figure 6D, middle panels). As judged by staining with monoclonal antibodies AE15 and AE13, inner root sheath and hair-shaft markers were absent (Figure 6E).

After an additional month, both the epidermis and residual permanent portion of embryonically established follicles had developed into large masses of relatively undifferentiated epithelial cells in the Tcf3-induced skin grafts (Figure 6D, right panels). The resulting skin epithelium lacked all major markers of terminal differentiation for epidermis, sebaceous glands, and hair follicles (Figure S3 and data not shown). However, these cells did express Sox9 (Figure 6E, right panels), which is an essential marker of bulge/ORS SCs important for their formation and/or maintenance (Vidal et al., 2005). Thus, Tcf3 expression seems to functionally promote features characteristic of skin progenitor cells as well as repress the three differentiation lineages afforded to them.

DISCUSSION

Tcf3, Wnt Signaling, and SC Maintenance

Our inducible Tcf3 system has yielded important new insights into how Tcf3 functions in skin progenitor cells. Consistent with our prior finding that Tcf3 acts as a transcriptional repressor in skin (Merrill et al., 2001), many affected genes were downregulated by Tcf3 induction. Since transgenic expression of constitutively stabilized β-catenin in Tcf3-positive bulge cells results in premature activation of the hair cycle (Lowry et al., 2005), one might have predicted that epidermal genes repressed by Tcf3 expression would be primarily cell-cycle regulated genes. Surprisingly, however, Tcf3-induced epidermal cells only repressed a few proliferation-associated genes, and this did not result in quiescence. Thus, if Tcf3 plays a role in slowing the cell cycle in the bulge, it does not seem to act on its own in this regard.

Although cell-cycle similarities between bulge and Tcf3-induced signatures were modest, the degree of overlap in signatures suggested that a number of bulge-cell characteristics are likely to be impacted by Tcf3. The relation between Tcf3 and progenitor status was further strengthened when we identified Tcf3 as a marker of embryonic skin progenitors and uncovered additional correlations between developmental expression patterns of Tcf3- and Tcf3-signature genes. We also uncovered similarities between the Tcf3 signature and that of the outer layer of the ORS, which is also thought to contain SCs (Oshima et al., 2001). Importantly, the similarities increased with time of Dox treatment, correlating with increasing levels of Tcf3. By contrast, the Tcf3-induced signature bore little resemblance to either epidermal or matrix signatures. Taken together, our results suggest that Tcf3 re-expression results in a reprogramming of postnatal epidermal cells to display a molecular signature that more closely resembles that of Tcf3-positive stem cells. Moreover, based upon our comparative analyses of the Tcf3-induced epidermal signature to endogenous Tcf3-positive skin stem cells, Tcf3 appears to be more closely linked to the progenitor status of the keratinocyte than its proliferative or Wnt-activation state.

Tcf3 as a Regulator of the Undifferentiated State of Skin Progenitor Cells

The quantitative inhibition of all three skin SC lineages by Tcf3 was both remarkable and unexpected. The repression was already evident within 6–48 hr of Tcf3 induction, but it was graphic in adult mice that expressed Tcf3 for longer time periods. In these animals, Tcf3 transformed the skin epithelium into masses of K5-positive, Sox9-positive keratinocytes with relatively undifferentiated morphology. Although intercellular adhesion and the epidermal-dermal border were still intact, molecular markers of epidermal, sebaceous gland, and hair follicle differentiation were repressed. The global inhibition of terminal differentiation pathways upon Tcf3 induction in vivo was particularly significant given our observation that Tcf3 is expressed not only in the bulge but also in the unspecified epidermal progenitor cells of embryonic skin. This relation was further paralleled by the developmental downregulation of Tcf3 as cell fates were determined. A final intriguing twist was our discovery that Tcf3 first appeared in embryonic hair follicles in a region that appears to mark the future site of the bulge, providing insights into when and how the skin epithelium might establish its reservoir of SCs for use in postnatal homeostasis and wound repair.

Overall, whether adult or embryonic and whether proliferating or quiescent, Tcf3 appears to be a characteristic of progenitor cells and incompatible with their ability to establish a terminally differentiating tissue. This newfound role for Tcf3 in maintaining an undifferentiated progenitor status may also explain why Tcf3 is restricted postnatally to bulge cells and is expressed albeit at reduced levels in the lower ORS cells, which retain certain features of their quiescent progenitors (Oshima et al., 2001; Vidal et al., 2005).

The Tcf3-PPAR Connection

Our microarray analyses exposed a key role for Tcf3 in repressing epidermal and sebaceous gland differentiation, which has not been implicated in canonical Wnt signaling. Notably, among the earliest genes to be affected by Tcf3 were *PPARγ* and *PPARα*, which were repressed shortly after Dox exposure both in vivo and in vitro. The rapidity of these changes and their dependency on Tcf3 was explained in part by the existence of Tcf/Lef1 regulatory elements in the endogenous *PPAR* promoters, which we showed bind Tcf3 directly in vitro as well as in vivo. Moreover, *PPARγ* reporter activity is also specifically repressed by Tcf3, as are the endogenous *PPARγ* and *PPARα* genes.

Although PPARs have long been known to regulate adipogenesis, their more general role in regulating secretory and lipid-related differentiation programs has only recently been realized (Di-Poi et al., 2004; Michalik et al.,

2002; Tontonoz et al., 1995). Interestingly, PPAR activities are often high in colon and other epithelial cancers where elevated levels of stabilized β-catenin are involved (Saez et al., 2004; Jansson et al., 2005). Our in vitro findings suggest that stabilized β-catenin can enhance *PPARγ* reporter gene activity and that this is dependent upon Tcf3. In this regard, it will be interesting in the future to evaluate whether Wnt signaling normally plays an active role in promoting sebaceous gland differentiation, or whether Tcf3 functions physiologically only in repressing this differentiation pathway in SCs.

CONCLUSIONS

Our results favor the view that Tcf3 functions in maintaining a certain program of relatively undifferentiated stratified epithelium that is characteristic of progenitor cells. Our finding further suggests that the activation and/or relief of Tcf3 target genes may be crutial for activating progenitor cells to enter differentiation programs in the skin. The particular lineage chosen by a progenitor cell appears to depend upon both intrinsic and extrinsic factors, and it need not necessarily involve canonical Wnt signaling. In hair cell fate specification, mesenchymal-epithelial interactions lead to a downregulation in Tcf3 expression and Wnt/β-catenin signaling. In embryonic skin development, other stimuli appear to be involved in the relief of Tcf3 repression and the concomitant induction of PPARγ in sebaceous gland specification and PPARα in epidermal differentiation. These findings underscore the importance of future studies aimed at understanding how Tcf genes are regulated during development and differentiation.

EXPERIMENTAL PROCEDURES

Generation and Analysis of Transgenic Mice

Transgenic mice were engineered as described (Vasioukhin et al., 1999). The SacI and HindIII fragment of *K14-rtTA* and the AattII and DrdI fragment of *TRE-mycTcf3* were used for injection (details of plasmid constructions are in Supplemental Data). For histology, dorsal backskins were fixed for preservation of lipids and embedded in Epon as described (Segre et al., 1999). Semithin sections (0.75 μm) were then stained with toluidine blue and counterstained with oil red O. IP injections of 100 μg Dox were administered to induce Tcf3. For Tcf3 expression beyond 3 days, mice were fed Dox-containing food (BIO-SERV, Frenchtown, NJ).

Skin grafts were performed as described (Kaufman et al., 2003). Skins from newborn *K14rtTA* or *K14rtTA/TRE-Tcf3* mice were grafted onto *Nude* mice, which were then placed on a Dox-containing diet. Skins were isolated for analyses after 27 days and 60 days post grafting.

Sample Preparation for Microarrays

P5 *K14rtTA* or *K14rtTA/TRE-Tcf3* mice were treated with Dox for 6, 12, and 24 hr to induce Tcf3. Backskins were harvested and treated with dispase at 37°C for 30 min to obtain epidermis. For P5 matrix, ORS, and basal epidermal cell arrays, we used *K14-H2B-GFP* transgenic mice (Tumbar et al., 2004). P5 Mx and ORS cells were isolated from hair-follicle preparations based on GFP levels as described (Rendl et al., 2005). For the isolation of Epi, the basal epidermal fractions from the same animals were isolated by surface α6 integrin and GFP.

RNAs were isolated by Trizol (Sigma) and then purified using RNAeasy minikits (Qiagen) and fluorometrically quantified (Ribogreen, Molecular Probes). Quality was assessed by RNA 6000 Pico Assay (Agilent), and 800 ng were primed with oligo(dT)-T7 and reverse transcribed (Superscript III cDNA synthesis kit; Invitrogen). One round of amplification/labeling was performed to obtain biotinylated cRNA (MessageAmp aRNA kit, Ambion), and 10 μg labeled cRNA was hybridized at 45°C for 16 hr to Affymetrix GeneChip Mouse Genome 430 2.0 arrays. Processed chips were read by an argon-ion laser confocal scanner (Genomics Core Facility, MSKCC).

Basal Cell Isolation and Purification

Backskins of E13.5 *K14-H2B-GFP* embryos and P5 neonatal mice were removed and incubated in 0.05% trypsin for 10 min at 37°C. Dissociated cells were removed of debris with cell strainers and subsequently stained with PE-conjugated α6 integrin antibody (red). Basal cells were FACS sorted on the basis of level of surface α6 and GFP.

Real-Time PCR

Total RNAs were purified as above, and after quantification with Ribogreen (Molecular Probes), normalized RNA quantities were reverse transcribed (Superscript III First-Strand Synthesis System, Invitrogen) using oligo(dT) primers. cDNAs were adjusted to equal levels by PCR amplification with primers to Gapdh. PCR amplifications of genes of interest were performed using, where possible, primers designed within the target sequences of the microarray probesets to ensure the uniqueness of the primers and amplicon. Amplifications with "minus reverse transcriptase" control cDNAs yielded no products for any of the primer pairs at the cycles tested. For real-time PCR, we used the LightCycler System (Roche), LightCycler 3.5 software, and the LightCycler DNA Master SYBR Green I reagents. Differences between samples and controls were calculated based on the $2^{-\Delta\Delta CP}$ method. Primer sequences used are listed in Table S3.

ChIP

ChIPs using primary epidermal MK were performed essentially as described (Chamorro et al., 2005, Lowry et al., 2005) . Both *K14rtTA* and *K14rtTA-mycTcf3* MK were induced, with 100 ng/ml Dox for 3 hr, prior to harvesting. In vivo ChIPs were done as described (Boyer et al., 2005) using protein A (Repligen) instead of magnetic beads. Skins from wild-type mice were treated with dispase to remove the epidermis, and the dermis was then treated with collagenase to remove the hair follicles (Rendl et al., 2005). ChIP lysates were then immunoprecipitated with the following Abs: guinea pig anti-Tcf3 (Fuchs lab), mouse anti-myc tag (Zymed), and guinea pig Igg or mouse Igg (Jackson Laboratory). Lef1/Tcf sites identified by rVista analysis of 5′ upstream sequences were defined by the ECR Browser and Ensemble software. Lef1/Tcf sites were chosen for ChIP analysis based on the conservation and alignment between mouse and at least one other species, including human, canine, and rat, and clustering of sites when applicable. As a control, PCR was also performed using primers that recognize other sites within the same promoter or downstream portions of these same genes to demonstrate the specificity of the pull-down. Primer sequences used are listed in Table S3.

Cell Culture and Retroviral Infections

MK were cultured in the presence of 15% serum and 0.3 mM $CaCl_2$ as described (Blanpain et al., 2004). Primary human keratinocytes (HKs) were grown in serum-free Epi-life media (Cascade Biologics). Transfections were done with low passage cells (≤5×). Retroviral stocks were produced by transfecting *Babe-PPARα* or *MSCV-PPARγ* in Phoenix cells and virus supernatants were collected 24 and 48 hr post transfection. Keratinocytes were infected, and after 48 hr, cells were harvested for RNAs, purified with Absolutely RNA Microprep kit (Stratagene). Transfections were with Fugene (Roche). Luciferase activity was measured with the Dual Luciferase Kit (Promega) with firefly luciferase values normalized to renilla-luciferase values.

Supplemental Data

Supplemental Data include six figures, three tables, and experimental procedures and can be found with this article online at http://www.cell.com/cgi/content/full/127/1/171/DC1/.

ACKNOWLEDGMENTS

We extend a special thank you to H. Amalia Passoli for conducting the ultrastrucural analyses presented in this paper. For generous gifts of reagents and Abs, we thank Wolfgang Hillen, Pierre Coulombe, and Hans Clevers. We thank the Rockefeller University core facility staff (Fred Quimby, LARC; Alison North, Bioimaging Facility; Agnes Viale, Juan Li, and Hui Zhao, Genomics Core Facility; Memorial Sloan Kettering Cancer Research Center), Fuchs' laboratory staff for technical assistance (Maria Nikolova, Lisa Polak, and Nicole Stokes), and the other members of the Fuchs lab for their genuine scientific curiosity and willingness to share ideas, reagents, and protocols. H.N. is the recipient of an NIH-NIAMS postdoctoral fellowship. E.F. is an investigator of the Howard Hughes Medical Institute. This work was supported in part by a grant R01 AR31737 from the NIH (E.F.).

Received: February 18, 2006
Revised: May 30, 2006
Accepted: July 31, 2006
Published: October 5, 2006

REFERENCES

Blanpain, C., Lowry, W.E., Geoghegan, A., Polak, L., and Fuchs, E. (2004). Self-renewal, multipotency, and the existence of two cell populations within an epithelial stem cell niche. Cell *118*, 635–648.

Boyer, L.A., Lee, T.I., Cole, M.F., Johnstone, S.E., Levine, S.S., Zucker, J.P., Guenther, M.G., Kumar, R.M., Murray, H.L., Jenner, R.G., et al. (2005). Core transcriptional regulatory circuitry in human embryonic stem cells. Cell *122*, 947–956.

Brannon, M., Brown, J.D., Bates, R., Kimelman, D., and Moon, R.T. (1999). XCtBP is a XTcf-3 corepressor with roles throughout Xenopus development. Development *126*, 3159–3170.

Cavallo, R.A., Cox, R.T., Moline, M.M., Roose, J., Polevoy, G.A., Clevers, H., Peifer, M., and Bejsovec, A. (1998). Drosophila Tcf and Groucho interact to repress Wingless signalling activity. Nature *395*, 604–608.

Chamorro, M.N., Schwartz, D.R., Vonica, A., Brivanlou, A.H., Cho, K.R., and Varmus, H.E. (2005). FGF-20 and DKK1 are transcriptional targets of beta-catenin and FGF-20 is implicated in cancer and development. EMBO J. *24*, 73–84.

Cotsarelis, G., Sun, T.T., and Lavker, R.M. (1990). Label-retaining cells reside in the bulge area of pilosebaceous unit: implications for follicular stem cells, hair cycle, and skin carcinogenesis. Cell *61*, 1329–1337.

Daniels, D.L., and Weis, W.I. (2005). Beta-catenin directly displaces Groucho/TLE repressors from Tcf/Lef in Wnt-mediated transcription activation. Nat. Struct. Mol. Biol. *12*, 364–371.

DasGupta, R., and Fuchs, E. (1999). Multiple roles for activated LEF/TCF transcription complexes during hair follicle development and differentiation. Development *126*, 4557–4568.

Day, T.F., Guo, X., Garrett-Beal, L., and Yang, Y. (2005). Wnt/beta-catenin signaling in mesenchymal progenitors controls osteoblast and chondrocyte differentiation during vertebrate skeletogenesis. Dev. Cell *8*, 739–750.

Di-Poi, N., Michalik, L., Desvergne, B., and Wahli, W. (2004). Functions of peroxisome proliferator-activated receptors (PPAR) in skin homeostasis. Lipids *39*, 1093–1099.

Gat, U., DasGupta, R., Degenstein, L., and Fuchs, E. (1998). De Novo hair follicle morphogenesis and hair tumors in mice expressing a truncated beta-catenin in skin. Cell *95*, 605–614.

Hamada, F., and Bienz, M. (2004). The APC tumor suppressor binds to C-terminal binding protein to divert nuclear beta-catenin from TCF. Dev. Cell *7*, 677–685.

Jansson, E.A., Are, A., Greicius, G., Kuo, I.C., Kelly, D., Arulampalam, V., and Pettersson, S. (2005). The Wnt/beta-catenin signaling pathway targets PPARgamma activity in colon cancer cells. Proc. Natl. Acad. Sci. USA *102*, 1460–1465.

Kang, S., Bajnok, L., Longo, K.A., Petersen, R.K., Hansen, J.B., Kristiansen, K., and MacDougald, O.A. (2005). Effects of Wnt signaling on brown adipocyte differentiation and metabolism mediated by PGC-1{alpha}. Mol. Cell. Biol. *25*, 1272–1282.

Kaufman, K.C., Zhou, P., Pasolli, H.M., Rendl, M., Bolotin, D., Lim, K., Dai, X., Alegre, M., and Fuchs, E. (2003). GATA-3: an unexpected regulator of cell lineage determination in skin. Genes Dev. *17*, 2108–2122.

Kim, C.H., Oda, T., Itoh, M., Jiang, D., Artinger, K.B., Chandrasekharappa, S.C., Driever, W., and Chitnis, A.B. (2000). Repressor activity of Headless/Tcf3 is essential for vertebrate head formation. Nature *407*, 913–916.

Kim, J.B., and Spiegelman, B.M. (1996). ADD1/SREBP1 promotes adipocyte differentiation and gene expression linked to fatty acid metabolism. Genes Dev. *10*, 1096–1107.

Knott, A., Garkle, K., Urlinger, S., Guthmann, J., Muller, Y., Thellman, M., and Hillen, W. (2002). Tetracycline-dependent gene regulation: combinations of transregulators yield a variety of expression windows. Biotechniques *32*, 796, 798, 800.

Korinek, V., Barker, N., Moerer, P., van Donselaar, E., Huls, G., Peters, P.J., and Clevers, H. (1998). Depletion of epithelial stem-cell compartments in the small intestine of mice lacking Tcf-4. Nat. Genet. *19*, 379–383.

Lee, H.-Y., Kleber, M., Hari, L., Brault, V., Suter, U., Taketo, M.M., Kemler, R., and Sommer, L. (2004). Instructive role of Wnt/{beta}-catenin in sensory fate specification in neural crest stem cells. Science *303*, 1020–1023.

Legg, J., Jensen, U.B., Broad, S., Leigh, I., and Watt, F.M. (2003). Role of melanoma chondroitin sulphate proteoglycan in patterning stem cells in human interfollicular epidermis. Development *130*, 6049–6063.

Lie, D.C., Colamarino, S.A., Song, H.J., Desire, L., Mira, H., Consiglio, A., Lein, E.S., Jessberger, S., Lansford, H., Dearie, A.R., and Gage, F.H. (2005). Wnt signalling regulates adult hippocampal neurogenesis. Nature *437*, 1370–1375.

Liu, J., and Farmer, S.R. (2004). Regulating the balance between peroxisome proliferator-activated receptor gamma and beta-catenin signaling during adipogenesis. A glycogen synthase kinase 3beta phosphorylation-defective mutant of beta-catenin inhibits expression of a subset of adipogenic genes. J. Biol. Chem. *279*, 45020–45027.

Lo Celso, C., Prowse, D.M., and Watt, F.M. (2004). Transient activation of beta-catenin signalling in adult mouse epidermis is sufficient to induce new hair follicles but continuous activation is required to maintain hair follicle tumours. Development *131*, 1787–1799.

Lowry, W.E., Blanpain, C., Nowak, J.A., Guasch, G., Lewis, L., and Fuchs, E. (2005). Defining the impact of beta-catenin/Tcf transactivation on epithelial stem cells. Genes Dev. *19*, 1596–1611.

Man, M.Q., Choi, E.H., Schmuth, M., Crumrine, D., Uchida, Y., Elias, P.M., Holleran, W.M., and Feingold, K.R. (2006). Basis for improved permeability barrier homeostasis induced by PPAR and LXR activators: liposensors stimulate lipid synthesis, lamellar body secretion, and post-secretory lipid processing. J. Invest. Dermatol. *126*, 386–392.

Merrill, B.J., Gat, U., DasGupta, R., and Fuchs, E. (2001). Tcf3 and Lef1 regulate lineage differentiation of multipotent stem cells in skin. Genes Dev. *15*, 1688–1705.

Merrill, B.J., Pasolli, H.A., Polak, L., Rendl, M., Garcia-Garcia, M.J., Anderson, K.V., and Fuchs, E. (2004). Tcf3: a transcriptional regulator of axis induction in the early embryo. Development *131*, 263274.

Michalik, L., Desvergne, B., Dreyer, C., Gavillet, M., Laurini, R.N., and Wahli, W. (2002). PPAR expression and function during vertebrate development. Int. J. Dev. Biol. *46*, 105–114.

Morris, R.J., Liu, Y., Marles, L., Yang, Z., Trempus, C., Li, S., Lin, J.S., Sawicki, J.A., and Cotsarelis, G. (2004). Capturing and profiling adult hair follicle stem cells. Nat. Biotechnol. *22*, 411–417.

Oshima, H., Rochat, A., Kedzia, C., Kobayashi, K., and Barrandon, Y. (2001). Morphogenesis and renewal of hair follicles from adult multipotent stem cells. Cell *104*, 233–245.

Rendl, M., Lewis, L., and Fuchs, E. (2005). Molecular dissection of mesenchymal–epithelial interactions in the hair follicle. PLoS Biol. *3*, e331.

Reya, T., and Clevers, H. (2005). Wnt signalling in stem cells and cancer. Nature *434*, 843–850.

Roose, J., Molenaar, M., Peterson, J., Hurenkamp, J., Brantjes, H., Moerer, P., van de Wetering, M., Destree, O., and Clevers, H. (1998). The Xenopus Wnt effector XTcf-3 interacts with Groucho-related transcriptional repressors. Nature *395*, 608–612.

Saez, E., Rosenfeld, J., Livolsi, A., Olson, P., Lombardo, E., Nelson, M., Banayo, E., Cardiff, R.D., Izpisua-Belmonte, J.C., and Evans, R.M. (2004). PPAR gamma signaling exacerbates mammary gland tumor development. Genes Dev. *18*, 528–540.

Schoonjans, K., Peinado-Onsurbe, J., Lefebvre, A.M., Heyman, R.A., Briggs, M., Deeb, S., Staels, B., and Auwerx, J. (1996). PPARalpha and PPARgamma activators direct a distinct tissue-specific transcriptional response via a PPRE in the lipoprotein lipase gene. EMBO J. *15*, 5336–5348.

Segre, J.A., Bauer, C., and Fuchs, E. (1999). Klf4 is a transcription factor required for establishing the barrier function of the skin. Nat. Genet. *22*, 356–360.

Shetty, P., Lo, M.C., Robertson, S.M., and Lin, R. (2005). C. elegans TCF protein, POP-1, converts from repressor to activator as a result of Wnt-induced lowering of nuclear levels. Dev. Biol. *285*, 584–592.

Sierra, J., Yoshida, T., Joazeiro, C.A., and Jones, K.A. (2006). The APC tumor suppressor counteracts β-catenin activation and H3K4 methylation at Wnt target genes. Genes Dev. *20*, 586–600.

Tachibana, K., Kobayashi, Y., Tanaka, T., Tagami, M., Sugiyama, A., Katayama, T., Ueda, C., Yamasaki, D., Ishimoto, K., Sumitomo, M., et al. (2005). Gene expression profiling of potential peroxisome proliferator-activated receptor (PPAR) target genes in human hepatoblastoma cell lines inducibly expressing different PPAR isoforms. Nucl. Recept. *3*, 3.

Taylor, G., Lehrer, M.S., Jensen, P.J., Sun, T.T., and Lavker, R.M. (2000). Involvement of follicular stem cells in forming not only the follicle but also the epidermis. Cell *102*, 451–461.

Tontonoz, P., Hu, E., Devine, J., Beale, E.G., and Spiegelman, B.M. (1995). PPAR gamma 2 regulates adipose expression of the phosphoenolpyruvate carboxykinase gene. Mol. Cell. Biol. *15*, 351–357.

Tumbar, T., Guasch, G., Greco, V., Blanpain, C., Lowry, W.E., Rendl, M., and Fuchs, E. (2004). Defining the epithelial stem cell niche in skin. Science *303*, 359–363.

van de Wetering, M., Sancho, E., Verweij, C., de Lau, W., Oving, I., Hurlstone, A., van der Horn, K., Batlle, E., Coudreuse, D., Haramis, A.P., et al. (2002). The beta-catenin/TCF-4 complex imposes a crypt progenitor phenotype on colorectal cancer cells. Cell *111*, 241–250.

van Es, J.H., Jay, P., Gregorieff, A., van Gijn, M.E., Jonkheer, S., Hatzis, P., Thiele, A., van den Born, M., Begthel, H., Brabletz, T., et al. (2005). Wnt signalling induces maturation of Paneth cells in intestinal crypts. Nat. Cell Biol. *7*, 381–386.

Van Mater, D., Kolligs, F.T., Dlugosz, A.A., and Fearon, E.R. (2003). Transient activation of beta catenin signaling in cutaneous keratinocytes is sufficient to trigger the active growth phase of the hair cycle in mice. Genes Dev. *17*, 1219–1224.

Vasioukhin, V., Degenstein, L., Wise, B., and Fuchs, E. (1999). The magical touch: genome targeting in epidermal stem cells induced by tamoxifen application to mouse skin. Proc. Natl. Acad. Sci. USA *96*, 8551–8556.

Vidal, V.P., Chaboissier, M.C., Lutzkendorf, S., Cotsarelis, G., Mill, P., Hui, C.C., Ortonne, N., Ortonne, J.P., and Schedl, A. (2005). Sox9 is essential for outer root sheath differentiation and the formation of the hair stem cell compartment. Curr. Biol. *15*, 1340–1351.

Willert, K., Brown, J.D., Danenberg, E., Duncan, A.W., Weissman, I.L., Reya, T., Yates, J.R., and Nusse, R. (2003). Wnt proteins are lipid-modified and can act as stem cell growth factors. Nature *423*, 448–452.